Articles

Synthesis and Reversible Redox Properties of an Electron-Rich Polyferrocenylsilane with *tert*-Butyl Substituents on the Cyclopentadienyl Ligands

Georgeta Masson,[†] Patrick Beyer,[†] Paul W. Cyr,[†] Alan J. Lough,[†] and Ian Manners*[,†,‡]

Department of Chemistry, University of Toronto, 80 St. George Street, Toronto, Ontario M5S 3H6, Canada, and School of Chemistry, University of Bristol, Bristol BS8 1TS, England

Received November 18, 2005; Revised Manuscript Received February 20, 2006

ABSTRACT: The strained sila-[1]ferrocenophane monomer Fe(η-$C_5H_3{}^tBu)_2SiPh_2$ (**5**) was synthesized and polymerized via thermal ring-opening polymerization (ROP) both in the melt and in solution to give the soluble high-molecular-weight polyferrocenylsilane (PFS) [Fe(η-$C_5H_3{}^tBu_2)_2SiPh_2]_n$, **7** ($M_n = 5.2 \times 10^4-1.7 \times 10^6$ Da, PDI = 1.38−1.99). Both monomer **5** and polymer **7** were structurally characterized by ^{1}H, ^{13}C, and ^{29}Si NMR spectroscopy and elemental analysis. The electronic structure and electrochemical properties of the monomer **5** and the polymer **7** were investigated by UV−vis spectroscopy and cyclic voltammetry. The oxidation potentials were shifted to more negative values relative to non-methylated or methylated analogues, indicating that the electron-donating effect of the ^{t}Bu group is transmitted to the iron center. Polymer **7** exhibited two reversible redox waves with a redox coupling, $\Delta E_{1/2}$, of 0.33 V, which is indicative of appreciable Fe···Fe interactions along the polymer backbone. The resiliency of **7** toward the redox processes was probed by measuring the molecular weights before photooxidation or chemical oxidation (with tetracyanoethylene (TCNE) or tris(4-bromophenyl)-ammoniumyl hexachloroantimonate) and after subsequent reduction of the oxidized polymers to the neutral forms by using bis(pentamethylcyclopentadienyl)iron(II). Significantly, unlike the previous studies of oxidized PFS homopolymers, soluble polymeric salts were obtained even for a high degree of oxidation, and these were characterized by UV−vis and IR spectroscopy. GPC measurements demonstrated the excellent redox resiliency of polyferrocenylsilane **7** to redox cycling as no appreciable decline in molecular weight was apparent for degrees of oxidation of up to 50%.

Introduction

The interest in metal-containing polymers has grown rapidly over the past decade due to their novel and useful characteristics that may allow a plethora of diverse applications.[1] Uses as functional components in nonlinear optical (NLO) devices and photocells,[2,3] catalysts,[4] redox-active gels,[5] photonic crystals,[6] nanostructured magnetic ceramics,[7] or liquid crystals[8] represent several examples. In addition, incorporating transition metals into self-organizing motifs such as block copolymers provides possibilities for the formation of supramolecular materials with novel properties.[4,9]

Polymetallocenes represent a well-established class of metallopolymers which are readily available via ring-opening polymerization (ROP) routes.[10] This method has been demonstrated to be applicable to a wide variety of metallocenophanes and related species to afford polymers incorporating different metals (e.g., Fe, Ru, Cr, Ti) and spacer elements (e.g., B, Si, Ge, Sn, P, S, Se, C_2).[11,12] The physical and chemical properties of polymetallocenes have been found to significantly depend on the bridging element and side groups.[1] Polyferrocenylsilanes (PFSs) **2**, the most well-studied examples of these materials, are accessible via thermal, transition-metal-catalyzed, anionic, and photolytic ROP of silicon-bridged [1]ferrocenophanes **1** (Scheme 1) as soluble materials with high molecular weights ($M_n > 10^5$ Da).[13,14]

Scheme 1

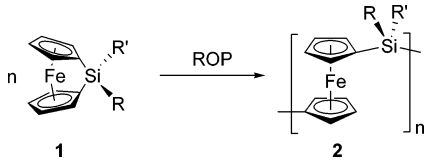

One of the most useful characteristics of PFS materials is their redox activity arising from the Fe^{II}/Fe^{III} couple. In contrast to the case of polyvinylferrocene, cyclic voltammetry has shown that PFSs exhibit two reversible redox waves of equal intensity.[15] These waves have been attributed to the oxidation of alternating iron centers at the first potential, $^1E_{1/2}$, followed by the oxidation of the iron centers in between at a higher potential, $^2E_{1/2}$. Thus, as one ferrocene unit in the polymer backbone is oxidized, the neighboring centers become more difficult to oxidize, and consequently, the two oxidation waves with redox coupling $\Delta E_{1/2} = {}^2E_{1/2} - {}^1E_{1/2}$ are obtained. The separation of the two waves, $\Delta E_{1/2}$, represents an approximate but useful measure of electronic interaction between iron centers in the polymer backbone.[16−18]

The studies of oxidized PFSs performed to date have demonstrated that these materials possess interesting properties.

* Corresponding author. E-mail: Ian.Manners@bristol.ac.uk.
† University of Toronto.
‡ University of Bristol.

10.1021/ma052475m CCC: $33.50
Published on Web 04/26/2006

Scheme 2

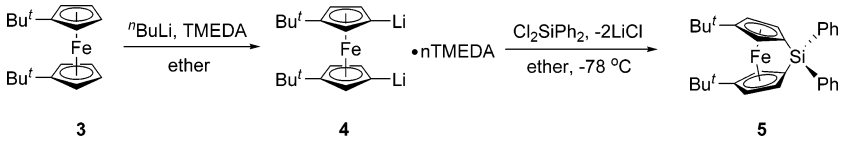

Scheme 3

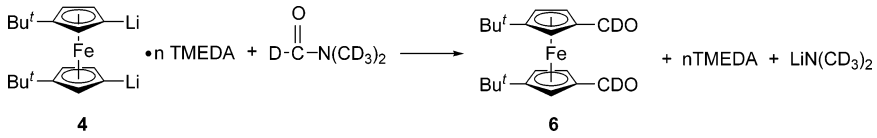

For example, the intrinsic conductivity of PFSs is very low (ca. 10^{-11} Ω^{-1} cm^{-1}), but upon vapor-phase oxidative doping with I_2, the conductivity of the polymer films increases up to 8 orders of magnitude relative to the unoxidized material.[19] More recently it has been shown[20] that irradiation of thin films of PFS cast from chloroform solution with UV light leads to photooxidation of ferrocene centers in the polymer main chain and to a considerable increase in conductivity. The photooxidized films also display significant photoconductivity,[21] a new characteristic for PFS materials. Unfortunately, dramatic molecular weight loss was detected after this photooxidation/reduction process. On the other hand, even the treatment of PFSs such as **2** (R = R′ = Me) with relatively mild nucleophilic species can lead to significant cleavage when degrees of oxidation exceed ca. 10%. This is likely a consequence of the appreciable lability of ferrocenium centers and nucleophilically induced iron−cyclopentadienyl (Fe−Cp) bond cleavage.[22] Moreover, oxidized PFS homopolymers have been found to be insoluble in nonnucleophilic organic solvents, which make these materials difficult to process and study.

The introduction of bulky electron-donating substituents to PFSs would be expected to afford materials with considerably improved resiliency toward redox cycling by lowering oxidation potentials, increasing Fe−Cp bond strength, and providing steric protection against nucleophilic attack. In addition, the introduction of such substituents on a polymer backbone represents one common approach to address potential insolubility problems.[23a,24] In this paper we report the synthesis and properties of PFS containing electron-donating and sterically demanding *tert*-butyl substituents on the cyclopentadienyl ligands and an investigation of their resiliency toward redox cycling.

Results and Discussion

Although the influence of the Si substituents on the properties of PFS materials has been well-studied,[25] the effect of substitution on the cyclopentadienyl (Cp) rings has been much less explored. It has been shown[26] that methylation of the Cp rings affects the character of the iron center and offers an alternative method for tuning electronic and optical properties of ferrocene-based polymers. With an increasing number of electron-donating methyl groups on the Cp rings, the oxidation potentials of methylated PFSs are shifted to more negative values, affording polymers which readily undergo electron-transfer reactions with mild oxidants such as TCNE, in contrast to the un-methylated analogues.

Trimethylsilyl substituents have also been successfully introduced into the Cp ligands of ferrocenophane monomers and ring-opened polymers.[27] Significantly, despite the steric bulk of Me_3Si groups, the polymerizability of the corresponding sila-[1]ferrocenophane was unaffected. However, Me_3Si groups have no significant effect on the oxidation potential of ferrocene units. The introduction of ^{t}Bu substituents was therefore explored due to the potentially favorable combination of steric bulk and electron-donating ability for improving redox resiliency.

1. Synthesis and Characterization of Fe(η-$C_5H_3{}^t$Bu)$_2$SiPh$_2$ (5). The starting material, 1,1′-di-*tert*-butyl ferrocene Fe(η-$C_5H_4{}^t$Bu)$_2$ (**3**), was synthesized following an adapted three-step literature procedure.[24] The preparation of the ^{t}Bu-substituted silicon-bridged ferrocenophane **5** required the initial synthesis of 1,1′-di-*tert*-butyl 3,3′-dilithioferrocene (**4**) by the reaction of **3** with ^{n}BuLi in hexanes or ether for 24 h at room temperature in the presence of *N*,*N*,*N*′,*N*′-tetramethylethylenediamine (TMEDA) as catalyst. Following a similar procedure to that reported by Compton and Rauchfuss[24] for the preparation of Fe(η-$C_5H_3{}^t$Bu)$_2S_3$, the one-pot synthesis of Fe(η-$C_5H_3{}^t$Bu)$_2$SiPh$_2$ (**5**) was attempted by adding $SiPh_2Cl_2$ at −78 °C to the complex **4** generated in situ (Scheme 2). However, we were unable to isolate significant quantities of the desired product **5** using this method.

To allow a more controlled synthesis of **5**, the orange precipitate **4** resulting from reaction of **3** with *n*-butyllithium was isolated in 42% yield as a pyrophoric powder. Because of the insolubility of **4** in common deuterated solvents, characterization by ^{1}H NMR was not possible. The ratio of the dilithio salt to TMEDA in complex **4** was determined by reaction with excess deuterated dimethylformamide (DMF), which led to the ferrocene dialdehyde derivative **6** and simultaneously released TMEDA (Scheme 3). On the basis of the integration of the signals corresponding to the −C(CH_3) groups from **6** and the −CH_3 groups from TMEDA in the ^{1}H NMR spectrum, it was determined that two molecules of TMEDA were released from one molecule of **4** in reaction with DMF. The excess of d_7-DMF served as a reference solvent for ^{1}H NMR analysis.

The synthesis of **5** was achieved by adding $SiPh_2Cl_2$ at −78 °C to a slurry of a known amount of **4** in ether, and **5** was isolated as a red-orange solid by low-temperature crystallization from hexanes. Further purification may be achieved by sublimation at 110−120 °C under vacuum (0.01 mmHg). Unlike most silicon-bridged [1]ferrocenophanes which are moisture sensitive,[28] **5** is air-stable and does not react with water or methanol in THF.

The identity of **5** was confirmed by ^{1}H, ^{13}C, and ^{29}Si NMR in addition to mass spectrometry and elemental analysis. The ^{1}H NMR spectrum showed one sharp singlet for the ^{t}Bu protons, three multiplet signals for the Cp rings, and two other multiplet signals for phenyl protons. The ^{13}C NMR spectrum exhibited 11 singlets: four attributed to phenyl groups, two for the ^{t}Bu groups, and five distinct resonances for Cp ligand. The Cp carbon atoms attached to the ^{t}Bu groups gave rise to a downfield resonance (112.20 ppm) relative to the conventional values of chemical shifts for Cp carbons (60−80 ppm), whereas the

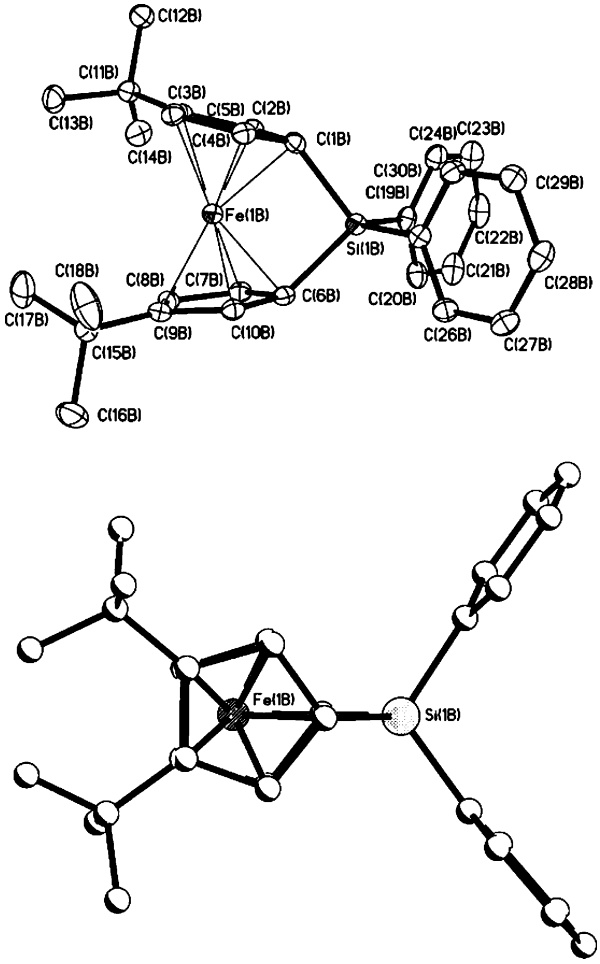

Figure 1. ORTEP views of **5** with thermal ellipsoids drawn at the 30% probability level. Hydrogen atoms have been omitted for clarity (top). The projection of the structure **5** showing the syn eclipsed conformation of the ^{t}Bu substituted Cp ligands (bottom).

carbon atoms attached to Si (C_{ipso}) displayed an upfield shift (29.7 ppm) which is characteristic of strained [1]ferrocenophanes.[23] Using CIGAR-HMBC spectroscopy,[29] it was possible to distinguish between the singlet of C_{ipso} and that of the quaternary carbon of ^{t}Bu (30.0 ppm). The ^{29}Si NMR spectrum of **5** showed a single resonance at −9.3 ppm, which indicated that the product consisted of a single ferrocenophane isomer, as confirmed by crystallographic analysis (see below).

2. X-ray Crystallographic Analysis of 5. To further characterize monomer **5**, single-crystal X-ray analysis was performed. Suitable single crystals of **5** for X-ray diffraction were obtained from a hexane solution after several days at −35 °C. Two molecules were found in the asymmetric unit having similar parameters. One molecule of hexane was found per four molecules of **5** in crystal lattice. The crystal structure confirmed the identity of **5** as a 3,3′-syn stereoisomer with a bent-sandwich geometry and eclipsed Cp rings (Figure 1).

The tilt angle α between the two Cp rings of 18.81° and the distorted tetrahedral geometry around the Si center (bond angle C(1)−Si−C(6): 98.30°) indicate the presence of significant ring strain which is comparable to that in the unsubstituted analogues Fe(η-C_5H_4)$_2$SiPh$_2$, **5a** (corresponding angles of 19.2° and 99.1°, respectively)[30] and methylated silicon-bridged [1]ferrocenophane, **5c** (18.6° and 96.96°, respectively).[31] These data prompted us to conclude that neither the increased electron-donating effect nor the bulkiness of the ^{t}Bu substituents induces significant structural changes in sila-[1]ferrocenophane molecules. Selected bonds lengths and angles for **5** are listed in Table 1.

Table 1. Summary of Key Structural Data for Ferrocenophane 5 (Bond Lengths in Å, Bond Angles in deg)

Si−C(1)	1.881(2)	Si−C(6)	1.891(2)
Si−C(19)	1.867(2)	Si−C(25)	1.858(2)
C3−C(11)	1.515(3)	C(9)−C(15)	1.520(3)
Fe displacement, Å	0.198(2)	Fe- - -Si	2.6645(6)
C(1)−Si−C(6)	98.30(9)	tilt angle, α	18.81
Cp−Si/Cp, β	39.5(2)	RC1−Fe−RC2,[a] δ	166.1(1)

[a] RC: ring centroid.

Table 2. UV−Vis Data for a Series of Ferrocenes and Sila-[1]ferrocenophanes[a]

compound	λ_{max} (nm)	ϵ (L^{-1} mol cm^{-1})	ref
Fe(η-C_5H_5)$_2$	440	100	32
Fe(η-C_5H_4Me)$_2$	438	161	31
Fe(η-$C_5H_4{}^tBu$)$_2$ (**3**)	441	160	this work
Fe(η-$C_5H_3{}^tBu$)$_2$SiPh$_2$ (**5**)	478	275	this work
Fe(η-C_5H_4)$_2$SiPh$_2$ (**5a**)	485	270	this work
Fe(η-C_5H_4)$_2$SiMe$_2$ (**5b**)	482	375	31
Fe(η-C_5H_3Me)$_2$SiMe$_2$ (**5c**)	476	372	31

[a] UV−vis data obtained for THF solutions.

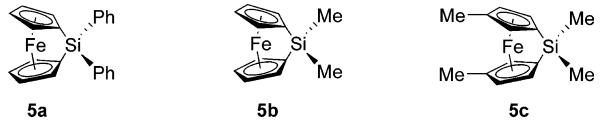

5a **5b** **5c**

3. UV−Vis and Cyclic Voltametry of [1]Ferrocenophane 5. We have investigated the electrochemical and electronic properties of **5** using cyclic voltammetry (CV) and UV−vis spectroscopy, respectively. These results are compared to those of **5a**, **5b**, and **5c**, obtained under identical experimental conditions.

The UV−vis spectrum of ferrocene and its derivatives has been studied extensively[32] and has led to the detection of six bands. Most studies of ferrocene-containing species have focused on band II at ca. 440 nm as in ferrocene itself, assigned to spin-allowed d−d transitions because it is the most intense in the visible region and well resolved. UV−vis data obtained from analysis of THF solutions of **5** indicated a λ_{max} of this band at 478 nm with a molar absorptivity of 275 L^{-1} mol cm^{-1}.

Therefore, similar to the strained sila-[1]ferrocenophane with methyl groups on the Cp rings **5c**[31] and unsubtituted analogues **5a**[30] and **5b**,[31] species **5** displays a bathochromic shift for band II accompanied by an increase of this band intensity relative to the analogous nonbridged species of ferrocene and di-*tert*-butylferrocene **3**. When compared to the unsubstituted analogue **5a**, the presence of electron-donating ^{t}Bu groups yields a very slight blue shift of band II in **5**. A similar blue shift was noted for **5b** and **5c** when Me groups are introduced to the Cp ligands. When the Ph groups on the Si atom in **5a** are replaced by Me groups (**5b**), a modest increase of extinction coefficient is noticed. The same behavior is observed for **5** and **5c** having electron-donating substituted Cp rings (Table 2).

Cyclic voltammetry was used in order to probe the electronic effect of the ^{t}Bu substituents on the iron center and the redox reversibility of **5**. The air and moisture stability of this ferrocenophane significantly facilitated the cyclic voltammetry (CV) studies. The CV trace of **5** in methylene chloride showed a reversible one-electron redox wave with an i_{red}/i_{ox} value close to unity, which indicates that the redox reaction is reversible on the CV time scale.[33]

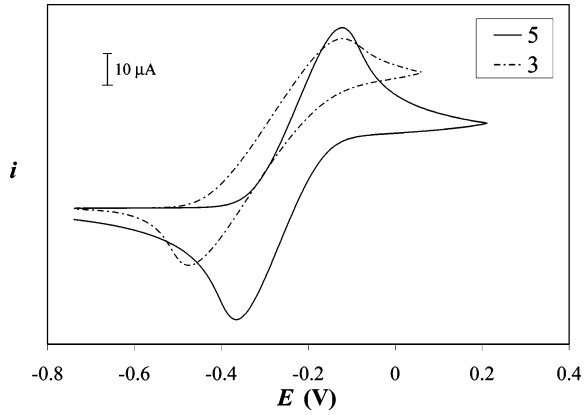

Figure 2. Cyclic voltammogram of CH_2Cl_2 solution of **3** and **5** vs ferrocene/ferrocenium ion couple (scan rate 100 mV/s).

It has been shown that the presence of methyl substituents in ferrocene[34] and ferrocenophane derivatives[31] reduces the half-wave oxidation potential by 50−55 mV per methyl group. As a ^{t}Bu group has a greater electron-donating effect than a methyl group, it was expected that the half-wave oxidation potential of **5** would be shifted to more negative values when compared to the analogous Cp methylated species **5c**. Indeed, the cyclic voltammogram obtained from analysis of a methylene chloride solution of **5** showed a half-wave potential, $E_{1/2}$, of −0.24 V vs the ferrocene/ferrocenium ion couple, whereas a value of −0.10 V was found for **5c**.[31] The cyclic voltammogram of **3** acquired under identical conditions showed a half-wave $E_{1/2}$ value of −0.30 V vs ferrocene/ferrocenium couple (Figure 2).[35a] This indicates that the electronic effect of the ^{t}Bu group is slightly less effectively transmitted to the iron center in **5** than in **3**.[35b]

4. Thermal Analysis of 5. DSC is a valuable tool that can be used to monitor the thermal ROP behavior of strained ferrocenophanes in order to determine optimal reaction conditions for bulk-scale thermal ROP. Generally, the DSC traces of strained ferrocenophanes show sharp melt endotherms followed by large broad exotherms assigned to the thermal ROP reaction.[23a,31] DSC is also useful to probe the effect of monomer structural changes on the ability to polymerize. Thus, it has been shown that increasing the number of the methyl groups on Cp from zero to eight in dimethylsila-[1]ferrocenophane induces a higher value of onset temperature in thermal ROP but does not significantly change the ROP enthalpy, $-\Delta H_p$ (70−80 kJ mol^{-1}). However, a decrease in ROP enthalpy to −60 kJ mol^{-1} was observed for **5a**.[23a]

Under identical experimental conditions (10 °C min^{-1} under N_2), DSC analysis was performed for **5** (Figure 3). The DSC trace for **5** showed two sharp endothermic peaks (at 134 and 157 °C) followed by a broad exotherm. The endothermic peak at 134 °C was assigned to solvent (hexane) loss from the crystal lattice since about 5% weight loss can be observed at this temperature by TGA. As noted above, hexane was used for recrystallization of **5** and was found in the crystal lattice by X-ray crystallographic analysis. The second endothermic peak at 157 °C was attributed to the melting process, which was immediately followed by a broad exotherm assigned to thermal ROP with an onset temperature around 190−210 °C. The area under the thermal ROP exotherm, representing $-\Delta H_p$, was found to correspond to ca. 40 kJ mol^{-1}, indicating a decrease of monomer polymerizability presumably due to the bulkiness of the *tert*-butyl and phenyl groups (Table 3). It is well-known that the bulky substituents serve to stabilize the cyclic forms relative to their ring-opened counterpart.[36]

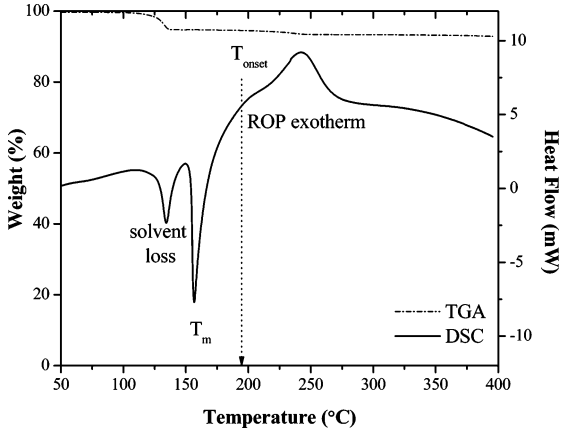

Figure 3. TGA trace (dotted line, scale left) and DSC thermogram (continuous line, scale right) for **5** obtained under N_2 at 10 °C min^{-1}.

Table 3. Thermal Analysis Data for Silicon-Bridged [1]Ferrocenophanes with Alkyl Groups on Cyclopentadienyl Rings and Unsubstituted Analogues

compound	T_m (°C)	T_{onset} (°C)	$-\Delta H_p$ (kJ mol^{-1})	ref
Fe(η-$C_5H_3{}^tBu)_2SiPh_2$ (**5**)	157	190	40	this work
Fe(η-$C_5H_4)_2SiPh_2$ (**5a**)	196	200	60	28
Fe(η-$C_5H_4)_2SiMe_2$ (**5b**)	98	107	80	25, 28
Fe(η-$C_5H_3Me)_2SiMe_2$ (**5c**)	113	122	73	25

Scheme 4

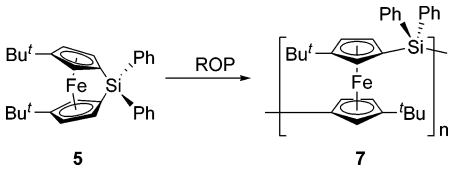

5. Ring-Opening Polymerization of 5. *Thermal ROP in Melt.* In a sealed evacuated glass tube, **5** was heated for 3 h at 250 °C. The contents of the tube became more viscous and finally immobile during this time.

The polyferrocenylsilane **7** that resulted from thermal ROP of **5** (Scheme 4) was isolated in 87% yield as a pink-orange powder by dissolution in THF followed by precipitation into methanol. In contrast to [Fe(η-$C_5H_4)_2SiPh_2]_n$,[23a] the PFS **7** is soluble in common organic solvents (THF, CH_2Cl_2, C_6H_6, toluene), allowing purification and complete characterization by GPC, ^{1}H, ^{13}C, and ^{29}Si NMR, and elemental analysis. A slight lower value for carbon percentage was determined by combustion methods compared with the calculated one. This is likely due to the formation of thermally stable C-rich ceramics on pyrolysis, which has ample precedent with PFS materials.[7]

A wide range of molecular weights and polydispersities (M_n = 5.2 × 10^4−1.7 × 10^6 Da, PDI = 1.38−1.99) were obtained by thermal ROP. The ^{1}H NMR spectrum of **7** showed characteristic broadening of the resonance relative to those of the monomer and slight changes in chemical shift. The ^{1}H NMR spectrum of **7** consists of three broad resonances due to Cp protons (3.95−4.16 ppm), a broad resonance assigned to the ^{t}Bu groups at 1.16 ppm, and two broad resonances due to the phenyl rings at 7.26 and 7.79 ppm. In the ^{13}C NMR spectrum of **7**, the upfield resonance for C_{ipso} observed in the strained monomer **5** (29.7 ppm) shifted to more conventional values for Cp carbons (br m 71.8 ppm). The ^{29}Si NMR spectrum consists of a single resonance at −11.7 ppm shifted slightly upfield compared to that of the monomer **5** (−9.3 ppm).

Thermal ROP in Solution. Xylene and decahydronaphthalene (Decalin) were considered as solvents for thermal ring-opening polymerization of **5** in solution. After refluxing a solution of **5** in xylene (bp 137−140 °C) for 24 h, only unreacted monomer was isolated. However, this is not surprising since the onset temperature found by DSC (around 190 °C) was not reached in this case. Performing an identical experiment in Decalin (bp 189−191 °C), high-molecular-weight polymer ($M_n = 9.1 \times 10^5$; PDI = 1.4) was isolated in 50% yield. The lower conversion is probably a result of the lower temperature used compared to melt polymerization (250 °C) and more dilute reaction conditions. Bimodal GPC curves were observed in some cases, and as in the case of thermal ROP in melt, molecular weights were found to vary over a wide range from one experiment to another. ^{1}H NMR analysis of the resulting polymer was consistent with that of the polymer synthesized by thermal ROP in melt.

Attempted Transition Metal Catalyzed ROP of 5. The polymerization of [1]ferrocenophanes in the presence of Rh^I, Pt^0, Pd^0, Pd^{II}, and Pt^{II} complexes as precatalyst has been extensively studied.[37] It was shown that the transition-metal-catalyzed ROP of silicon-bridged [1]ferrocenophanes permits control of regiostructure and also the molecular weight by using Et_3SiH as a capping agent. Furthermore, access to novel PFSs with graft, star, and block architecture was possible using commercially available Si−H functionality sources.[38]

We attempted ROP of **5** using Karstedt's catalyst (a (divinyltetramethyldisiloxane)platinum(0) complex in xylenes), $PtCl_2$, and [Rh(1,5-cod)$_2$]OTf under a wide variety of conditions. Only low-molecular-weight oligomers were isolated in very low yield (0−7%), although ^{1}H NMR analysis of reaction mixture indicated 95% conversion of the monomer into ring-opened species based on the integration of the phenyl groups.

Attempted Anionic and Photolytic Anionic Ring-Opening Polymerization (PROP) of 5. Under mild conditions (25 °C, in THF) in the presence of anionic initiators such as ^{n}BuLi, highly purified silicon-bridged [1]ferrocenophanes undergo ROP.[39] This allows the synthesis of polymers with controlled molecular weights and narrow polydispersity. End-functionalized polymers and the first block copolymers containing skeletal transition metal atoms were also prepared via this method.[40] More recently, a new living ROP mechanism for sila-[1]ferrocenophanes involving the Fe−Cp cleavage by the use of a moderately nucleophilic initiator such as M[C_5H_4R] (where M = Li or Na and R = ^{t}Bu, Me, or H) under UV irradiation was discovered in our group.[41] The latter approach involves Fe−Cp bond cleavage, and it is fundamentally different from living anionic ROP, which involves Si−Cp cleavage induced by attack of an organolithium species at Si. This method may represent an alternative route for ROP of strained [1]ferrocenophanes with strerically hindered Si−Cp bonds as is the case in **5**. However, both attempted anionic and photolytic anionic ROP led only to oligomeric species, which were isolated in poor yield (0−10%). It is assumed that a mechanism involving a buildup of negative charge on the Cp rings such as that in anionic or photolytic anionic ROP may be less favored in the case of **5** where the ^{t}Bu groups already endow increased electron density on the Cp ligands.

6. Thermal Analysis of PFS 7. Thermal analysis of PFSs has previously shown that T_g is strongly dependent on the side groups at silicon.[25] As well, a smooth increase of T_g with increasing number of methyl substituents on the Cp ring has been observed. DSC analysis of **7** indicated a glass transition with a small change in heat capacity and a temperature around 210 °C. No melting transition was observed up to 350 °C. The high value of T_g (Figure 4) was expected considering the effect of the rigid and bulky substituents such as *tert*-butyl and phenyl upon the polymer chain flexibility.

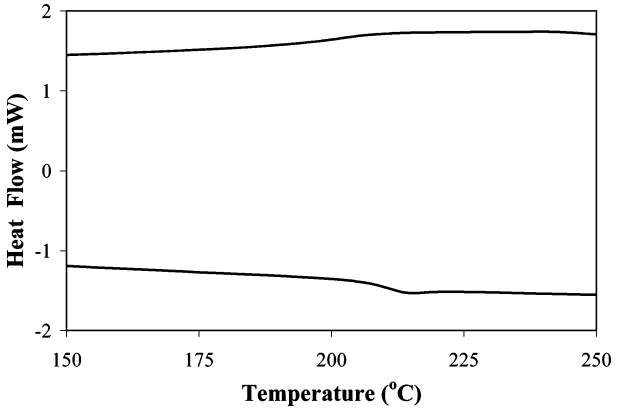

Figure 4. DSC thermogram of **7** obtained under N_2 at 10 °C min^{-1}.

Table 4. Thermal Analysis Data for a Series of Polyferrocenylsilanes

polymer	T_g[a] (°C)	T_{10}[b] (°C)	T_{50}[b] (°C)	ref
[Fe(η-$C_5H_3{}^tBu)_2SiPh_2]_n$ (**7**)	212	440	510	this work
[Fe(η-$C_5H_3Me)_2SiMe_2]_n$	73	390	460	25
[Fe(η-$C_5H_4)_2SiMe_2]_n$	33	430	520	25

[a] Obtained by DSC analysis at 10 °C min^{-1} under N_2. [b] Obtained by TGA at 10 °C min^{-1} under N_2.

When heated under an inert atmosphere (N_2), PFSs are stable up to 350 °C before they suffer weight loss to afford stable Fe/Si/C ceramic materials at 600−1000 °C. It was found that **7** is thermally stable up to 320 °C, with a subsequent rapid degradation through 600 °C. The ceramic yield at 1000 °C was about 25%. For comparative purposes, Table 4 summarizes the temperatures corresponding to 10% (T_{10}) and 50% (T_{50}) weight loss from TGA traces and glass transition temperature (T_g) data for **7** and previously reported values for PFS obtained from **5b** and **5c**.

7. UV−Vis and Cyclic Voltammetry of PFS 7. The electron-donating effect of the ^{t}Bu groups attached to each Cp ring on the ferrocene units in polymer backbone was investigated using cyclic voltammetry and UV−vis spectroscopy.

As with the corresponding monomer spectrum, our UV−vis analysis of the polymer **7** focused on band II (at 440 nm in ferrocene). Analysis of PFS **7** in THF solution revealed the maximum absorption for this band at 460 nm with a molar absorptivity of 210 L^{-1} mol cm^{-1}, which is consistent with previous findings showing that ROP of strained ferrocenophanes results in a blue shift to values closer to that of ferrocene (440 nm).

The electrochemistry of PFSs is characterized by two reversible redox waves with a peak separation in the range 0.20−0.25 V, depending slightly on the substituents present at silicon. As previously shown,[26] with increasing number of methyl groups on the Cp rings, both first and second oxidation waves shift to lower oxidation potentials without affecting the wave separation.

The CV of **7** (Figure 5) displayed the expected two reversible oxidation waves with $^1E_{1/2} = -0.32$ V at the first wave and $^2E_{1/2} = 0.01$ V at the second wave relative to the ferrocene/ferrocenium ion couple. The electron-donating effect of the ^{t}Bu groups is transmitted to the iron center, and the separation between the two waves, $\Delta E_{1/2}$, of value 0.33 V for **7** indicates an Fe···Fe interaction in the polymer backbone comparable with that in biferrocene (0.34 V) where the ferrocene units are directly

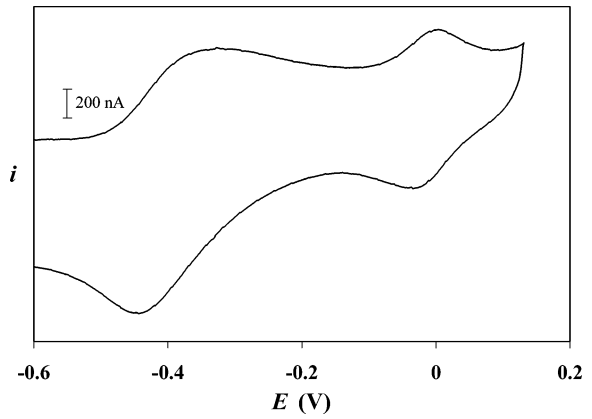

Figure 5. Cyclic voltammogram of CH_2Cl_2 solution of **7** vs ferrocene/ferrocenium ion couple (scan rate 100 mV/s).

Table 5. Redox-Coupling Values for a Series of Ferrocene-Containing Polymers[a]

polymer	$^1E_{1/2}$ (V)	$^2E_{1/2}$ (V)	$\Delta E_{1/2}$ (V)	ref
$[Fe(\eta\text{-}C_5H_3{}^tBu)_2\ SiPh_2]_n$ (**5**)	−0.32	0.01	0.33	this work
$[Fe(\eta\text{-}C_5H_3{}^tBu)_2S_2]_n$	0.64	0.93	0.29	24
$[Fe(\eta\text{-}C_5H_3Me)_2SiMe_2]_n$	−0.16	0.04	0.20	25
$[Fe(\eta\text{-}C_5H_4)_2SiMe_2]_n$	−0.03	0.17	0.20	25

[a] Data are obtained by analysis at 22 °C of CH_2Cl_2 solutions and referenced to the ferrocene/ferrocenium ion couple.

Scheme 5

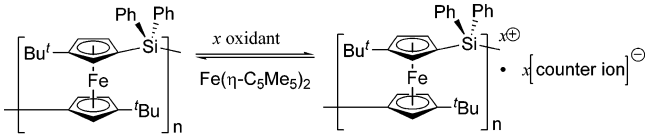

7 **7$^+$a**

linked. A similar effect was observed by Rauchfuss[24] in poly(ferrocenylene persulfides) with ^{t}Bu-substituted Cp rings where the S−S spacers are as effective in promoting Fe···Fe interactions as a single SiR_2 spacer in PFSs with no alkyl substituents on the Cp rings. Table 5 lists the comparative values of the half-wave potential and the redox coupling for a series of polyferrocenes.

8. Photooxidation and Chemical Oxidation of PFS 7. As shown by the electrochemical studies described above, the electron-donating effect of the ^{t}Bu groups on the Cp rings is effectively transmitted to iron as the first wave oxidation potential is shifted to more negative values. Next, we undertook studies to test the resiliency of **7** in photooxidation and chemical oxidation processes.

(a) Photooxidation of PFS 7 in the Presence of Chloroform Vapor. The preparation of the films, experimental conditions, and UV−vis measurements were carried out in identical conditions as previously reported[20] for PFS derivatives. Following oxidation, bis(pentamethylcyclopentadienyl)iron(II), Fe(η-C_5Me_5)$_2$, with a formal potential of −0.59 V in methylene chloride vs ferrocene/ferrocenium couple,[42] was used as a convenient and clean reducing agent. The reactions are represented in Scheme 5.

As in previous work,[20] the polymer degradation was quantified by the number of cleavages per chain, $N_{sc} = [M_n(\text{before})/M_n(\text{after}) - 1]$. Unfortunately, using polymer **7** in photooxidation experiments affords no improvement toward polymer degradation (Table 6). Neither the electron-donating effect nor the steric hindrance of the bulky ^{t}Bu groups led to the increased

Table 6. Molecular Weight Loss after One Photooxidation/Reduction Cycle on PFSs Films

polymer	M_n, Da (PDI) before oxidation[a]	M_n, Da (PDI) after reduction[b]	N_{sc}
$[Fe(\eta\text{-}C_5H_4)_2SiMe_2]_n$	2.2×10^5 (2.25)	2.1×10^4 (1.89)	9[c]
$[Fe(\eta\text{-}C_5H_3Me)_2SiMe_2]_n$	7.3×10^4 (1.94)	1.2×10^4 (2.25)	5[c]
$[Fe(\eta\text{-}C_5H_3{}^tBu_2)_2SiPh_2]_n$ (**7**)	3.1×10^4 (2.28)	3.4×10^3 (5.32)	8

[a] PFS films exposed to UV irradiation for 60 min in the presence of $CHCl_3$ vapor. [b] PFS film reduced with Fe(η-C_5Me_5)$_2$ solution. [c] Reference 20.

Scheme 6

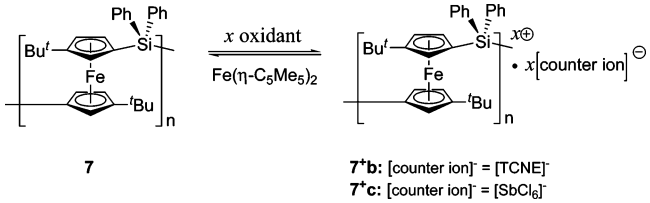

7 **7$^+$b:** [counter ion]$^-$ = [TCNE]$^-$ **7$^+$c:** [counter ion]$^-$ = [$SbCl_6$]$^-$

stability of these materials during the photooxidation process. These results suggest that the polymer chain cleavage upon photooxidation is apparently induced by highly reactive chlorinated photoproducts rather then redox instability of the oxidized polymer (see Scheme 5), as was initially proposed.[20]

(b) Chemical Oxidation of PFS 7. The redox reactions represented in Scheme 6 were studied with the aim of further exploring the stability of the oxidized polymer **7**$^{x+}$.

Reaction with Tetracyanoethylene. The low oxidation potential of the first redox wave in **7** indicates that this polymer should be easier to oxidize than Cp methylated analogues. Addition of 1.00 and 0.50 equiv of TCNE to solutions of PFS **7** resulted in darkening of the reaction mixtures. The half-wave oxidation potential of TCNE, −0.21 V vs ferrocene/ferrocenium couple, was determined by cyclic voltammetry in methylene chloride solution under identical experimental conditions as for **7** (see Experimental Section). The reaction products were isolated by precipitation in hexanes as pale-green materials. In each case, the resulting polymeric salt **7**$^{x+}$**b** was redissolved in CH_2Cl_2, and UV−vis and FT-IR spectra were acquired. The optical spectrum of untreated polymer **7** showed the d−d transitions band at 460 nm in CH_2Cl_2, whereas the UV−vis spectrum of the product obtained with TCNE displayed an additional band around 660 nm ascribed to the ligand-to-metal charge transfer (LMCT) transition, characteristic of ferrocenium centers.[43] However, the fraction of ferrocenium cations was roughly estimated using the known extinction coefficients for ferrocene and ferrocenium cation[32] and was found to be much lower than expected (about 10%). Incomplete oxidation is to be expected considering the relatively close $E_{1/2}$ values of the first oxidation wave of **7** and that of TCNE.

IR spectroscopy has been proved to be very useful in determining the oxidation state of many possible forms of TCNE in its charge-transfer state.[44] None of the characteristic bands for $[TCNE]^-$, $[TCNE]^{2-}$, or $[TCNE]_2^{2-}$ were detected in the IR spectrum of **7**$^{x+}$**b**. Instead, a single −C≡N vibration appeared at 2199 cm^{-1}, which has been also observed previously in products derived from PFS oxidation with TCNE.[14f,26] Independent of the number of equivalents of TCNE added to PFS **7** (0.50 or 1.00), the IR spectrum of the residue remaining after solvent removal indicates the presence of the ν(C≡N) characteristic bands in neutral TCNE (2221 and 2259 cm^{-1}) which, in agreement with UV−vis spectroscopy findings, signaled the incomplete oxidation reaction.

Rereduction using Fe(η-C_5Me_5)$_2$ as a reducing agent allowed the isolation of a pink-orange material with the ^{1}H NMR and UV−vis spectra identical with those of the pristine polymer. GPC measurements before oxidation ($M_n = 6.2 \times 10^4$ Da; PDI = 1.35) and after rereduction ($M_n = 4.5 \times 10^4$ Da; PDI = 1.42) indicated no significant changes in molecular weight ($N_{sc} < 1$).

Reaction with Tris(4-bromophenyl)ammoniumyl Hexachloroantimonate. Tris(4-bromophenyl)ammoniumyl hexachloroantimonate, $[N(C_6H_4Br\text{-}4)_3]^+[SbCl_6]^-$ (Magic Blue), with a formal oxidation potential of 0.70 V vs ferrocene/ferrocenium ion couple in CH_2Cl_2[42] was chosen as a stronger one-electron oxidant compared to TCNE. Although silver salts are widely used as stoichiometric reagents in iron(II) oxidation, colloidal silver is formed and difficult to remove. Triarylaminium radical cations, on the other hand, are able to cleanly oxidize the ferrocene derivatives as the byproduct resulting from electron-transfer reaction, $N(C_6H_4Br\text{-}4)_3$, is colorless, facilitating UV−vis investigations on the oxidized products without further purification.[45]

A series of oxidation reactions were performed for various molar ratio, *x*, of added Magic Blue to monomeric units [Fe(η-$C_5H_3{}^tBu)_2SiPh_2$] in **7**: 0.10, 0.25, 0.50, 0.75, and 1.00. Considering the much higher oxidation potential of Magic Blue than both the first and second oxidation waves of **7**, the molar fraction of ferrocenium cations resulting from the oxidation process was expected to be proportional to the molar ratio, *x*. The solutions of the resulting polymeric salts, $\mathbf{7}^{x+}\mathbf{c}$, remained stable indefinitely, allowing accurate UV−vis investigations. This represents a significant result as the other appreciably oxidized PFS homopolymers reported to date were insoluble in common organic solvents. The UV−vis spectrum of each solution showed the expected d−d band at 460 nm and also a LMCT band at 660 nm, indicating the presence of ferrocenium centers. With increasing molar ratio of Magic Blue one additional broad band developed in the electronic spectra of $\mathbf{7}^{x+}\mathbf{c}$ at 1350 nm (Figure 6a). This new band observed in the NIR region, which is observed in mixed-valence compounds,[46] is assigned to intervalence charge transfer (IT) and represents evidence for electron delocalization and considerable interaction between the Fe(II) and Fe(III) centers.[15b] The intensity of the LMCT band increased linearly with the amount of added triarylaminium salt up to 0.5 mol equiv, demonstrating that the fraction of ferrocenium ions formed is proportional to the number of moles of the added oxidizing agent (Figure 6b). In contrast, beyond 0.5 equiv of added oxidant, no significant increase was observed in the LMCT band intensity. As the oxidant should be fully capable of completely oxidizing **7** based on redox potentials, this suggests that polymer chain cleavage may occur on attempted generation of a fraction of ferrocenium centers higher than 0.5.

After rereduction using Fe(η-C_5Me_5)$_2$, ^{1}H NMR and UV−vis spectra as well as GPC measurements were obtained for the neutral polymers isolated by precipitation in methanol. In all cases, ^{1}H NMR showed identical spectra to the pristine unoxidized polymer **7**, and no LMCT band around 660 nm was observed by UV−vis spectroscopy, suggesting complete conversion of ferrocenium units to ferrocene moieties. GPC measurements after one redox cycle using $[N(C_6H_4Br\text{-}4)_3]^+[SbCl_6]^-$ as oxidant and Fe(η-C_5Me_5)$_2$ as reductant indicated good resiliency toward the redox cycle for a molar ratio, *x*, up to 0.5 (see Table 7). However, considerable molecular weight loss was observed for *x* values higher than 0.5, supporting the assumption of polymer chain cleavage based on the optical spectroscopy findings. It is worth noting that the counterion may also play an important role in polymer degradation as $[SbCl_6]^-$ may be a source of $SbCl_5$ or nucleophilic chloride ions which could cleave the Fe(III)−Cp bonds as it has also been observed in organic chemistry.[47,48] In addition, hydrolysis of $[SbCl_6]^-$ by traces of moisture could generate HCl, which could also lead to cleavage of Fe−Cp bonds.

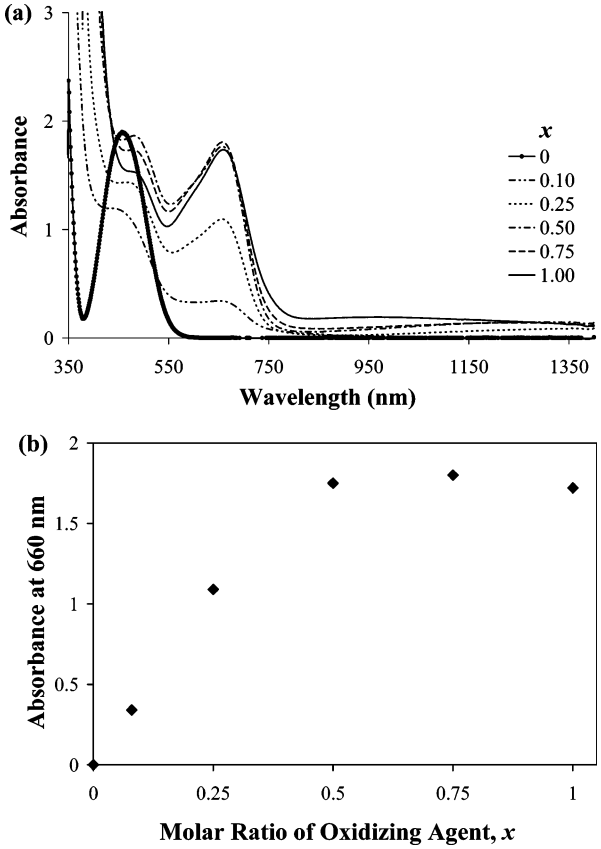

Figure 6. (a) UV−vis spectra of $\mathbf{7}^{x+}\mathbf{c}$ in CH_2Cl_2 for various molar ratios, *x*, of $[N(C_6H_4Br\text{-}4)_3]^+[SbCl_6]^-$ as oxidizing agent. (b) Dependence of absorbance of LMCT band on the molar ratio of the oxidizing agent.

Table 7. Molecular Weight Loss of 7 after One Redox Cycle Using Various Molar Ratios of Oxidizing Agent

	M_n, Da (PDI)		
x	before oxidation	after reduction	N_{sc}
0.10	5.2×10^4 (1.38)	4.3×10^4 (1.41)	0
0.25	5.2×10^4 (1.38)	2.9×10^4 (1.31)	<1
0.50	5.2×10^4 (1.38)	1.6×10^4 (1.44)	2
>0.75	5.2×10^4 (1.38)	7.1×10^3 (2.03)[a]	6−7

[a] The M_n value for a 0.75 molar ratio of added $[N(C_6H_4Br\text{-}4)_3]^+[SbCl_6]^-$ is given as a typical example.

Summary

Diphenylsila-[1]ferrocenophane **5** with ^{t}Bu substituents on the Cp rings was successfully synthesized and completely characterized. The corresponding high-molecular-weight PFS **7** was obtained by thermal ROP in the melt and in solution. Unlike the diphenyl sila-PFS material without substituents on the Cp ring, polymer **7** is highly soluble in common organic solvents, allowing complete characterization. The negative shift of the first oxidation potential observed by cyclic voltammetry indicated that the electron-donating effect of the *tert*-butyl substituents is transmitted to the iron centers. Neither the increased stability of the Fe−Cp bond due to the *tert*-butyl

electron-donating effect nor the bulkiness of the substituents could prevent polymer degradation during photooxidation. This behavior, along with previous reported studies, prompted us to conclude that molecular weight loss is induced by highly reactive chlorinated photoproducts. Oxidation reactions using TCNE or $[N(C_6H_4Br\text{-}4)_3]^+[SbCl_6]^-$ led to soluble polymeric salts even for high degrees of oxidation. The process was found to be reversible by using $Fe(\eta\text{-}C_5Me_5)_2$ as reductant and was monitored spectroscopically. The presence of oxidized iron centers in the polymer backbone gave rise to a band at 660 nm in the UV−vis spectra. A broad IT band to much higher wavelength (1300 nm) which signals a mixed-valence material also developed with increased molar ratio of $[N(C_6H_4Br\text{-}4)_3]^+[SbCl_6]^-$. In was shown that good resiliency toward redox cycling is achieved for **7** for up to 0.5 mol equiv of added oxidant. On the basis of the two-step oxidation process operating for PFS materials, this indicates that in this study instability arises when two nearest-neighbor ferrocenium sites are created. Further improvements in the stability of oxidized PFS materials will probably require the use of more inert counterions than $[SbCl_6]^-$ used in the present work.

Experimental Section

Materials. Most reactions and manipulations were carried out under an atmosphere of prepurified nitrogen gas (BOC) using common Schlenk techniques or an inert atmosphere glovebox (M-Braun). Solvents were dried using a Grubbs-type solvent system[49] or standard methods followed by distillation. The materials were purchased from Aldrich except $PtCl_2$, Karstedt's catalyst, and Et_3SiH purchased from Gelest Inc. In some cases the reagents were purified by distillation. TCNE was sublimed in a vacuum prior to use. 6,6-Dimethylfulvene and $^tBuC_5H_4Li$ were prepared according to literature procedures.[24]

Equipment. ^1H (400 MHz), ^{13}C (100.5 MHz), and ^{29}Si (79.5 MHz) NMR spectra were recorded on a Varian Unity 400 spectrometer. The 2-D NMR spectrum was obtained using a Varian Inova 500 spectrometer. ^1H and ^{13}C resonances were referenced internally to the deuterated solvent resonances, and ^{29}Si resonances were referenced to $SiMe_4$ resonances utilizing a normal pulse sequence. Solid-state ^{13}C NMR spectra were recorded at 50 MHz, and solid-state ^{29}Si NMR spectra (CP/MAS) were recorded at 79.5 MHz on a Bruker DSX 400 spectrometer, with $Si(SiMe_3)_4$ (−9.9 ppm referenced to TMS) as an external chemical shift reference. Mass spectra were obtained with the use of a VG 70-250S mass spectrometer operating in electron impact (EI) mode. Elemental analyses were performed at the University of Toronto using a Perkin-Elmer 2400 series C/H/N analyzer. Molecular weights were determined by gel permeation chromatography (GPC) using a Viscotek GPC MAX liquid chromatograph equipped with a Viscotek triple detector array. The triple detector array consists of a deflection refractometer, a four-capillary differential viscometer, and a right angle laser light scattering detector ($\lambda_0 = 670$ nm). The triple detector has been shown to provide absolute molecular weight values for PFS homopolymers, and we assume that it provides accurate value of M_w/M_n.[50] Conventional calibration was also used, and molecular weights were determined relative to polystyrene standards purchased from American Polymer Standards. In both cases, a flow rate of 1.0 mL/min was used with ACS grade tetrahydrofuran as the eluent. Ultraviolet−visible spectra were recorded using a Perkin-Elmer Lambda 900 UV−vis−NIR spectrometer. Polymer molar absorptivity was quoted per monomer repeating unit. Infrared spectra were recorded using a Perkin-Elmer Spectrum One FT-IR spectrometer. Photolysis of **5** was performed with a Philips 125 W high-pressure mercury arc lamp. A Pyrex filter was placed inside the quartz immersion well to filter out wavelengths below 310 nm. Thermal analysis of **5** was performed on a TA Instruments simultaneous DSC−TGA (SDT) Q600 at a heating/cooling rate of 10 °C min^{-1} under N_2. DSC experiments for polymer **7** were performed on a TA Instruments DSC2920 at a heating/cooling rate of 10 °C min^{-1} under N_2. Thermogravimetric analysis of **7** was performed at heating rate of 10 °C min^{-1} under N_2 using a TA Instruments modulated thermogravimetric analyzer Q500. Cyclic voltammetry was performed using an Epsilon EC instrument equipped with an Au electrode and an Ag/AgCl reference electrode. The working electrode, Au, was used in conjunction with a Pt wire as counter electrode. Data are obtained by analysis at 22 °C of CH_2Cl_2 solutions with a concentration of 5×10^{-3} M in monomer or polymer and 0.1 M in $[NBu_4][PF_6]$ at a scan rate of 100 mV/s. CH_2Cl_2 was previously dried over CaH_2 and distilled. $[NBu_4][PF_6]$ was previously recrystallized from EtOH and vacuum-dried. Ferrocene was added as internal standard at the end of the experiments, and potentials are reported vs the ferrocene/ferrocenium ($E = 0.00$ V).

Synthesis of 3. This procedure was adapted from that of Rauchfuss.[24] A 1 L Schlenk flask was charged with 30.00 g of ^{t}BuCpLi (0.234 mmol) and dissolved in ca. 300 mL of dry THF. Separately, about 200 mL of THF was added to 15.15 g of $FeCl_2$, 98% purity (117 mmol), and the resulted suspension was transferred over ^{t}BuCpLi solution at 0 °C. The resulting brown-red suspension was allowed to warm to room temperature and then refluxed for 12 h. After the removal of the THF, the dark brown residue was diluted with ca. 100 mL of hexanes (LiCl insoluble) and filtered through a 3−5 cm pad of silica gel. The evaporation of the solvent gave a red oily product which ^1H NMR indicated to comprise **3** as the major product; 22.6 g (65%) of the highly pure product was obtained by crystallization at −60 °C from a concentrated solution in hexanes.

^1H NMR (400 MHz, C_6D_6, 25 °C): δ 4.01 (m, 4H, Cp-*H*), 3.94 (m, 4H, Cp-*H*), 1.22 (s, 18 H, C*CH*$_3$). $^{13}C\{^1H\}$ NMR (100.5 MHz, C_6D_6, 25 °C): δ 101.2 (*Cp*^{t}Bu), 67.43, 65.0 (*Cp*H), 31.5 (C*C*H$_3$), 30.3 (*C*CH$_3$).

Synthesis of 4. In a 500 mL Schlenk flask 22 g (0.074 mol) of $^tBu_2fc$ was dissolved in 250 mL of dry ether. 22.3 mL of TMEDA (0.148 mmol) was then added via syringe. The solution was cooled to 0 °C, and 92.5 mL of ^{n}BuLi solution 1.6 M in hexanes were added dropwise over 20 min. After removal of the ice bath, stirring was continued for 24 h at room temperature. The red solution darkened after a few minutes, and an orange precipitate was formed after 24 h. The supernatant was decanted, and the orange solid was washed with 3−4 portions of 100 mL of hexanes and dried under vacuum. This gave 17 g of an orange, pyrophoric powder (42% assuming two molecules of TMEDA in complex **4**).

Synthesis of 5. To a suspension of 3.8 g of **4** (7.0 mmol) in 150 mL of dry diethyl ether neat distilled $SiCl_2Ph_2$ (1.6 mL, 10.0 mmol, 1.1 equiv) was added dropwise via syringe at −78 °C. The reaction was allowed to warm to room temperature and continued for 3 h. Ether was removed under reduced pressure, and the resulting dark red viscous liquid was dissolved in 100 mL of hexanes. The precipitated LiCl was removed by filtration through Celite on a filter frit. The volume of the clear red solution was reduced to ca. 20 mL and kept at −60 °C overnight, resulting in deposition of a red-orange precipitate. The supernatant was decanted, and the product recrystallized from concentrated solution at −60 °C. To achieve the purity requested by anionic ring-opening polymerization when no spurious peaks appear in the ^1H NMR spectrum with vertical scale increased 10 times relative to the C*CH*$_3$ (s, 1.13 ppm) peak, further purification was performed by sublimation under vacuum (0.01 mmHg) at 100−120 °C. 1.2 g (36%) of highly pure product was isolated. Attempts to synthesize other silicon-bridged [1]ferrocenophanes having ^{t}Bu-substituted Cp rings via the reaction of **4** with $RR'SiCl_2$ (R = R′ = Me; R = Me, R′ = Ph; R = Me, R′ = Cl) led to very low yields of pure products. These species were not further studied.

^1H NMR (400 MHz, C_6D_6, 25 °C): δ 8.12 (d, $^3J_{HH} = 8.1$, 4 H, *ortho-Ph*), 7.23−7.19 (m, 6 H, *meta* and *para-Ph*), 4.33 (m, 2H, Cp-*H*), 4.18 (m, 2H, Cp-*H*), 4.16 (m, 2H, Cp-*H*), 1.13 (s, 18H, C*CH*$_3$). $^{13}C\{^1H\}$ NMR (100.5 MHz, C_6D_6, 25 °C): δ 135.40, 134.3, 130.2, 128.4 (−*Ph*), 112.3 (*Cp*^{t}Bu), 76.2, 75.4, 73.3 (*Cp*H), 31.7 (C*C*H3), 30.0 (*C*CH$_3$), 29.7 (*ipso-Cp*). $^{29}Si\{^1H\}$ NMR (79.4 MHz, C_6D_6, 25 °C): δ −9.3. MS (70 eV, EI): *m*/*z* (%) 480 (14) [M +

2]$^+$, 479 (46) [M + 1]$^+$, 478 (100) [M]$^+$, 463 (18) [M-CH_3]$^+$, 406 (17) [M−CH_3−C(CH_3)$_3$]$^+$, 57 (17) [C(CH_3)$_3$]$^+$. HRMS (70 eV, EI): calcd for $C_{30}H_{34}{}^{56}$FeSi 478.53246; found 478.2597. Anal. Calcd for $C_{30}H_{34}$FeSi: C, 75.30; H, 7.16. Found: C, 75.01; H, 7.59; mp 157 °C (DSC). UV−vis (25 °C, THF): λ_{max} = 478 nm, ϵ (L^{-1} mol cm^{-1}) = 275.

Synthesis of PFS 7. (i) Thermal ROP in Melt. 150 mg (0.31 mmol) of **5** were flame-sealed in an evacuated (0.01 mmHg) glass Pyrex tube and heated at 250 °C for 3 h. The red melt became more viscous and finally immobile. The tube content was dissolved in THF, filtered, and then precipitated in methanol. The pink-orange solid was reprecipitated (THF/methanol), collected by filtration, and dried in vacuo to afford 130 mg of polymer (87% yield).

^{1}H NMR (C_6D_6, 400 MHz, 25 °C): δ 7.79 (br s, 4 H, *ortho-Ph*), 7.26 (br s, 6 H *meta* and *para-Ph*), 4.13 (br m, 4H, Cp-*H*), 3.96 (br s, 2H, Cp-*H*), 1,16 (br s, 18H, CC*H*$_3$). Solid-state ^{13}C NMR (50.3 MHz, 25 °C): δ 136.7, 128.2 (br m, −*Ph*), 107.0 (br m, *Cp*^{t}Bu), 71.8 (br m, *Cp*). Solid-state ^{29}Si NMR (79.5 MHz, spin rate 8 kHz, 25 °C): δ −11.7. GPC (triple detection): M_n = 1.7 × 10^6 Da, PDI (M_w/M_n) = 1.37 (molecular weights vary in a wide range from an experiment to another: M_n = 1.7 × 10^6−5.2 × 10^4 Da, PDI = 1.37−1.99). Anal. Calcd $C_{30}H_{34}$FeSi: C, 75.31; H, 7.11. Found: C, 73.52; H, 7.40. UV−vis (25 °C, THF): λ_{max} = 460 nm, ϵ (L^{-1} mol cm^{-1}) = 210.

(ii) Thermal ROP in Solution. A solution of **5** (150 mg, 0.31 mmol) in xylene (0.8 mL) was stirred at reflux (bp 137−140 °C). After 24 h no polymerization was observed by ^{1}H NMR. A similar experiment was carried out in decahydronaphthalene (Decalin; bp 189−191 °C). After 4 h of refluxing the reaction solution was allowed to cool, and 75 mg (50%) of polymer was isolated by precipitation in methanol followed by filtration. The ^{1}H NMR spectrum is consistent with that of polymer **7** obtained by thermal ROP in melt. GPC (triple detection): M_n = 9 × 10^5 Da, PDI (M_w/M_n) = 1.40.

Attempted Synthesis of PFS 7 Using Transition-Metal Catalysis. The following standard procedure is typical. A solution of **5** (96 mg, 0.20 mmol) in toluene (1 mL) was treated with Karstedt's catalyst (1 mol %) at room temperature under stirring. The extent of reaction was monitored by ^{1}H NMR spectroscopy, and 50% monomer conversion was attained after 24 h. By raising the temperature to 60 °C, 95% monomer conversion was observed after 3 h by ^{1}H NMR spectroscopy. A pink-orange powder was isolated in a poor yield (6%) by precipitation into methanol. A similar procedure was used for the attempted ROP of **5** under various reaction conditions (concentration, solvent, temperature, catalyst). Et_3SiH was also used as capping agent in attempting the synthesis of polymers with controlled molecular weight. Only oligomeric species were isolated in yields varying from 0 to 10%. Besides, ^{1}H NMR data were consistent with that of polymer **7** obtained by thermal ROP in melt. GPC (triple detection): M_n = 3.0 × 10^3 Da, PDI = 1.07.

Attempted Synthesis of PFS 7 by Anionic ROP. A solution of **5** (120 mg, 0.25 mmol) in THF (0.5 mL) was treated at room temperature with ^{n}BuLi (16 μL, 1.6 M in hexanes 0.025 mmol) under vigorous stirring. After 2 h, the reaction was quenched with a few drops of degassed water, and a pink-orange product was isolated in poor yield (10%) by precipitation in methanol. Besides characteristic ^{1}H NMR resonances found for **7**, ^{n}Bu end groups were also observed.

Selected ^{1}H NMR data: 1.33 (br m, 2H, SiCH$_2$C*H*$_2$CH$_2$CH$_3$), 1.26 (br m, 2H, SiCH$_2$CH$_2$C*H*$_2$CH$_3$), 1.07 (br m, 2H, Si*CH*$_2$CH$_2$-CH$_2$CH$_3$), 0.88 (br m, 3H, SiCH$_2$CH$_2$CH$_2$C*H*$_3$. GPC (triple detection): M_n = 2.0 × 10^3 Da, PDI = 1.04.

Attempted Synthesis of PFS 7 by Photolytic ROP. A solution of **5** (96 mg, 0.2 mmol) in THF (0.5 mL) was treated at room temperature with 10 μL of Li[C_5H_4Me] 2 M solution in the absence of light. The solution has been irradiated for 3 h with UV light under stirring at 5 °C and quenched with few drops of degassed water. No product was isolated by precipitation in methanol. After solvent removal, the ^{1}H NMR spectrum indicated the presence of monomer as the major component.

Table 8. Crystal Data and Structure Refinement for 5

empirical formula	C31.50 H37.50 Fe Si
formula weight	500.05
temp, K	150(1)
wavelength, Å	0.710 73
crystal system	triclinic
space group	$P\bar{1}$
a, Å	12.7472(2)
b, Å	13.0861(2)
c, Å	17.0006(3)
α, deg	81.869(1)
β, deg	74.488(1)
γ, deg	83.991(1)
Z	4
ρ_{calc}, g cm^{-1}	1.231
μ(Mo Kα), mm^{-1}	0.620
F(000)	1066
crystal size, mm^3	0.26 × 0.16 × 0.04
θ range, deg	2.57−27.58
reflections collected	35505
independent reflections	12347 (R_{int} = 0.0575)
absorption correction	semiempirical from equivalents
max and min transmission coeff	0.977 and 0.925
GoF on F^2	1.024
$R1^a$ ($I > 2\sigma(I)$)	0.0410
$wR2^b$ (all data)	0.1051
peak and hole, e·Å^{-3}	0.401 and −0.405

^{a} $R1 = \sum||F_0| - |F_c||/\sum|F_0|$. ^{b} $wR2 = \{\sum[w(F_0^2 - F_c^2)^2]/\sum[w(F_0^2)^2]\}^{1/2}$.

Oxidation of PFS 7 with TCNE and Subsequent Treatment with Bis(pentamethylcyclopentadienyl)iron(II). 10 mL solution of TCNE in dichloromethane (14 mg, 0.11 mmol) was added with stirring to 10 mL CH_2Cl_2 solution of PFS **7** (48 mg, 0.10 mmol of monomer units) with M_n = 6.2 × 10^4 Da and PDI = 1.35 (determined by conventional GPC relative to polystyrene standards). The reaction solution visibly darkened within 1 h, and the color changed from red to brown. After 24 h, the reaction mixture was split into two portions. The first portion was filtered, and a UV−vis spectrum was acquired. The resulting pale-green solid obtained by solvent removal was dried under vacuum and investigated by UV−vis and FT-IR. The neutral polymer was recovered by treating the second portion of the reaction mixture with an excess of Fe(η-C_5Me_5)$_2$. After 2 h, the polymer solution was concentrated, and a pink-orange product was isolated by precipitation in methanol. This product was found to be identical to pristine polymer **7** by ^{1}H NMR. A similar procedure was applied for a 0.5 molar ratio of TCNE:monomer unit so that the reaction mixture had the same concentration in monomer units. GPC (conventional calibration), after reduction with Fe(η-C_5Me_5)$_2$: M_n = 4.5 × 10^4 Da, PDI = 1.42. UV−vis (25 °C, THF): λ_{max} = 460 nm, 660 nm. FT-IR (25 °C, Nujol), ν(C≡N): 2199 (s), 2221 (s), 2259 cm^{-1} (s).

Oxidation of PFS 7 with Tris(4-bromophenyl)ammoniumyl Hexachloroantimonate and Subsequent Treatment with Bis-(pentamethylcyclopentadienyl)iron(II). The following standard procedure for oxidation of 10 mol % of the ferrocene units in **7** by using a corresponding amount of [N(C_6H_4Br-4)$_3$]$^+$[$SbCl_6$]$^-$ as a one electron oxidant is typical. Similarly, a series of experiments involving 0.25, 0.50, 0.75, and 1.00 mol equiv of [N(C_6H_4Br-4)$_3$]$^+$-[$SbCl_6$]$^-$ were carried out so that the reaction mixture had the same concentration in monomer units. The red color of polymer solutions changed within the first hour to light green or dark green depending on the molar ratio of the added oxidizing agent.

1 mL of 5 × 10^{-3} M CH_2Cl_2 solution of [N(C_6H_4Br-4)$_3$]$^+$-[$SbCl_6$]$^-$ was added with stirring to 10 mL CH_2Cl_2 solutions of **7** (24 mg, 0.05 mmol of monomer units) having M_n = 5.2 × 10^4 Da and PDI = 1.38 (determined by conventional GPC relative to polystyrene standards). After 24 h no precipitate formation was observed, and the UV−vis spectrum of the polymeric salt solution was acquired. The reaction mixture was split into two portions. The first was immediately concentrated, and the reaction product was isolated by precipitation in hexane (the polymeric salt is soluble in methanol). The resulting green material was washed with 2−3

portions of 10 mL of hexanes, dried under vacuum, and redissolved in CH_2Cl_2. A UV−vis spectrum of this solution showed the same absorption bands as the spectrum recorded for the aliquot from reaction mixture. The neutral polymer was recovered by treating the second portion of reaction mixture with an excess of Fe(η-C_5Me_5)$_2$. After 2 h, the polymer solution was concentrated, and a pink-orange product was isolated by precipitation in methanol. This product was found to be identical to pristine polymer **7** by ^{1}H NMR. GPC (conventional calibration), after reduction with Fe(η-C_5Me_5)$_2$: $M_n = 4.3 \times 10^4$ Da, PDI = 1.41. UV−vis (25 °C, THF): $\lambda_{max} = 460$ nm, 660 nm, 1300 nm (for mol equiv higher than 0.25).

X-ray Crystallography. Single-crystal X-ray diffraction data were collected using a Nonius Kappa-CCD diffractometer and monochromated Mo Kα radiation ($\lambda = 0.710\,73$ Å) and were measured using a combination of ϕ scans and ω scans with κ offsets to fill the Ewald sphere. The data were processed using the Denzo-SMN package.[51] The structure was solved and refined using SHELXTL V6.1[52] for full-matrix least-squares refinement that was based on F^2. All H atoms were included in calculated positions and allowed to refine in riding-motion approximation. Selected data for investigated compound **5** are given in Table 8. The supplementary crystallographic data for this paper can be obtained free of charge via the Internet at www.ccdc.cam.ac.uk/conts/retrieving.html (or from the Cambridge Crystallographic Data Centre,12 Union Road, Cambridge CB2 1EZ, U.K.).

Acknowledgment. We thank Wing Yan Chan for help and useful discussions and Dr. Timothy Burrow for collecting 2-D NMR data. P.B. thanks the D.A.A.D (Germany) for fellowship support. I.M. thanks the Canadian Government for a Research Chair, the EU for a Marie Curie Chair, and the Royal Society for a Wolfson Research Merit Award.

References and Notes

(1) (a) Manners, I. *Synthetic Metal-Containing Polymers*; Wiley-VCH: Weinheim, 2004. (b) Abd-El-Aziz, A. S., Carraher, C. E., Jr., Pittman, C. U., Jr., Sheats, J. E., Zeldin, M., Eds.; *Macromolecules Containing Metal and Metal-Like Elements, Vol. 2: Organoiron Polymers*; John Wiley & Sons, Inc.: Hoboken, NJ, 2004. (c) Schubert, U. S.; Eschbaumer, C. *Angew. Chem., Int. Ed.* **2002**, *41*, 2892. (d) Nguyen, P.; Gomez-Elipe, P.; Manners, I. *Chem. Rev.* **1999**, *99*, 1515.

(2) (a) Leung, A. C. W.; Chong, J. H.; MacLachlan, M. J. *Macromol. Symp.* **2003**, *196*, 229. (b) Wong, W.-Y.; Lu, G.-L.; Choi, K.-H.; Shi, J.-X. *Macromolecules* **2002**, *35*, 3506. (c) Wright, M. E.; Toplikar, E. G.; Lackritz, H. S.; Kerney, J. T. *Macromolecules* **1994**, *27*, 3016. (d) Davey, A. P.; Page, H.; Blau, W.; Byrne, H. J.; Cardin, D. J. *Synth. Met.* **1993**, *57*, 3980. (e) Guha, S.; Frazier, C. C.; Porter, P. L.; Kang, K.; Finberg, S. E. *Opt. Lett.* **1989**, *14*, 952.

(3) Garo, K., Ed.; *Nonlinear Optical Properties of Organic Materials*; Proc. SPIE No. 971; The International Society for Optical Engineering: Washington, DC, 1988; p 186.

(4) (a) Lastella, S.; Jung, Y. J.; Yang, H.; Vajtai, R.; Ajayan, P. M.; Ryu, C. Y.; Rider, D. A.; Manners, I. *J. Mater. Chem.* **2004**, *14*, 1791. (b) Hinderling, C.; Keles, Y.; Stöckli, T.; Knapp, H. F.; de los Arcos, T.; Oelhafen, P.; Korczagin, I.; Hempenius, M. A.; Vancso, G. J.; Pugin, R.; Heinzelmann, H. *Adv. Mater.* **2004**, *16*, 876. (c) Durkee, D. A.; Eitouni, H. B.; Gomez, E. D.; Ellsworth, M. W.; Bell, A. T.; Balsara, N. P. *Adv. Mater.* **2005**, *17*, 2003.

(5) (a) Kulbaba, K.; MacLachlan, M. J.; Evans, C E. B.; Manners, I. *Macromol. Chem. Phys.* **2001**, *202*, 1768. (b) Bu, H.-z.; English, A. M.; Mikkelsen, S. R. *J. Phys. Chem. B* **1997**, *101*, 9593. (c) Tatsuma, T.; Takada, K.; Matsui, H.; Oyama, N. *Macromolecules* **1994**, *27*, 6687. (d) Sykora, M.; Maxwell, K. A.; Meyer, T. J. *Inorg. Chem.* **1999**, *38*, 3596.

(6) (a) Arsenault, A. C.; Halfyard, J.; Wang, Z.; Kitaev, V.; Ozin, G. A.; Manners, I.; Mihi, A.; Miguez, H. *Langmuir* **2005**, *21*, 499. (b) Arsenault, A. C.; Miguez, H.; Kitaev, V.; Ozin, G. A.; Manners, I. *Adv. Mater.* **2003**, *15*, 503.

(7) (a) Ginzburg, M.; MacLachlan, M. J.; Yang, S. M.; Coombs, N.; Coyle, T. W.; Raju, N. P.; Greedan, J. E.; Herber, R. H.; Ozin, G. A.; Manners, I. *J. Am. Chem. Soc.* **2002**, *124*, 2625. (b) Massey, J. A.; Winnik, M. A.; Manners, I.; Chan, V. Z. H.; Ostermann, J. M.; Enchelmaier, R.; Spatz, J. P.; Möller, M. *J. Am. Chem. Soc.* **2001**, *123*, 3147. (c) Kulbaba, K.; Resendes, R.; Cheng, A.; Bartole, A.; Safa-Sefat, A.; Coombs, N.; Stöver, H. D. H.; Greedan, J. E.; Ozin, G. A.; Manners, I. *Adv. Mater.* **2001**, *13*, 732.

(8) (a) Steffen, W.; Köhler, B.; Altmann, M.; Scherf, U.; Stitzer, K.; zur Loye, H.-C.; Bunz, U. H. F. *Chem.—Eur. J.* **2001**, *7*, 117. (b) Turpin, F.; Guillon, D.; Deschenaux, R. *Mol. Cryst. Liq. Cryst.* **2001**, *362*, 171. (c) Wilbert, G.; Traud, S.; Zentel, R. *Macromol. Chem. Phys.* **1997**, *198*, 3769. (d) Liu, X.-H.; Bruce, D. W.; Manners, I. *Chem. Commun.* **1997**, *3*, 289. (e) Hagihara, N.; Sonogashira, K.; Takahashi, S. *Adv. Polym. Sci.* **1981**, *41*, 149.

(9) (a) Kim, K. T.; Vandermeulen, G. W. M.; Winnik, M. A.; Manners, I. *Macromolecules* **2005**, *38*, 4958. (b) Wang, X.-S.; Winnik, M. A.; Manners, I. *Angew. Chem., Int. Ed.* **2004**, *43*, 3703. (c) Manners, I. *Science* **2001**, *294*, 1664.

(10) Manners, I. *Polyhedron* **1996**, *15*, 4311.

(11) (a) Vogel, U.; Lough, A. J.; Manners, I. *Angew. Chem., Int. Ed.* **2004**, *43*, 3321. (b) Berenbaum, A.; Manners, I. *Dalton Trans.* **2004**, *14*, 2057. (c) Resendes, R.; Nelson, J. M.; Fischer, A.; Jäkle, F.; Bartole, A.; Lough, A. J.; Manners, I. *J. Am. Chem. Soc.* **2001**, *123*, 2116. (d) Berenbaum, A.; Braunschweig, H.; Dirk, R.; Englert, U.; Green, J. C.; Jäkle, F.; Lough, A. J.; Manners, I. *J. Am. Chem. Soc.* **2000**, *122*, 5765. (e) Rulkens, R.; Gates, D. P.; Balaishis, D.; Pudelski, J. K.; McIntosh, D. F.; Lough, A. J.; Manners, I. *J. Am. Chem. Soc.* **1997**, *119*, 10976.

(12) (a) Tamm, M.; Kunst, A.; Bannenberg, T.; Herdtweck, E.; Sirsch, P.; Elsevier, C. J.; Ernsting, J. M. *Angew. Chem., Int. Ed.* **2004**, *43*, 5530. (b) Mochida, K.; Shibayama, N.; Goto, M. *Chem. Lett.* **1998**, 339. (c) Mizuta, T.; Onishi, M.; Miyoshi, K. *Organometallics* **2000**, *19*, 5005.

(13) Kulbaba, K.; Manners, I. *Macromol. Rapid Commun.* **2001**, *22*, 711.

(14) For the work of other group on polyferrocenylsilanes and related materials: (a) Pannell, K. H.; Imshennik, V. I.; Maksimov, Yu. V.; Il'ina, M. N.; Sharma, H. K.; Papkov, V. S.; Suzdalev, I. P. *Chem. Mater.* **2005**, *17*, 1844. (b) Péter, M.; Lammertink, R. G. H.; Hempenius, M. A.; Vancso, G. J. *Langmuir* **2005**, *21*, 5115. (c) Kloninger, C.; Rehahn, M. *Macromolecules* **2004**, *37*, 8319. (d) Shi, W.; Cui, S.; Wang, C.; Wang, L.; Zhang, X.; Wang, X.; Wang, L. *Macromolecules* **2004**, *37*, 1839. (e) Eitouni, H. B.; Balsara, N. P. *J. Am. Chem. Soc.* **2004**, *126*, 7446. (f) Tang, H.; Liu, Y.; Chen, X.; Qin, J.; Inokuchi, M.; Kinoshita, M.; Jin, X.; Wang, Z.; Xu, B. *Macromolecules* **2004**, *37*, 9785. (g) Hmyene, M.; Yasser, A.; Escorne, M.; Perche-on-Guegen, A.; Garnier, F. *Adv. Mater.* **1994**, *6*, 564. (h) Tanaka, M.; Hayashi, T. *Bull. Chem. Soc. Jpn.* **1993**, *66*, 334.

(15) (a) Nishihara, H. *Adv. Inorg. Chem.* **2002**, *53*, 41. (b) Rulkens, R.; Lough, A. J.; Manners, I.; Lovelace, S. R.; Grant, C.; Geiger, W. E. *J. Am. Chem. Soc.* **1996**, *118*, 12683. (c) Nguyen, M. T.; Diaz, A. F.; Dement'ev, V. V.; Pannell, K. H. *Chem. Mater.* **1994**, *6*, 952.

(16) (a) Jones, S. C.; Barlow, S.; O'Hare, D. *Chem.—Eur. J.* **2005**, *11*, 4473. (b) Barrière, F.; Camire, N.; Geiger, W. E.; Mueller-Westerhoff, U. T.; Sanders, R. *J. Am. Chem. Soc.* **2002**, *124*, 7262.

(17) Southard, G. E.; Curtis, D. M. *Organometallics* **2001**, *20*, 508.

(18) Brown, G. M.; Meyer, T. J.; Cowan, D. O.; LeVanda, C.; Kaufman, F.; Roling, P. V.; Rausch, M. D. *Inorg. Chem.* **1975**, *14*, 506.

(19) (a) Espada, L.; Pannell, K. H.; Papkov, V.; Leites, L.; Bukalov, S.; Suzdalev, I.; Tanaka, M.; Hayashi, T. *Organometallics* **2002**, *21*, 3758. (b) Rulkens, R.; Resendes, R.; Verma, A.; Manners, I.; Murti, K.; Fossum, E.; Miller, P.; Matyjaszewski, K. *Macromolecules* **1997**, *30*, 8165.

(20) Cyr, P. W.; Tzolov, M.; Manners, I.; Sargent, E. H. *Macromol. Chem. Phys.* **2003**, *204*, 915.

(21) Tzolov, M.; Cyr, P. W.; Sargent, E. H.; Manners, I. *J. Chem. Phys.* **2004**, *120*, 1990.

(22) For example, treatment of polyferrocenylsilanes such as [Fe(η-C_5H_4)$_2$-$SiMe_2$]$_n$ with oxidants such as $[N(C_6H_4Br\text{-}4)_3]^+[SbCl_6]^-$ leads to molecular weight decline, which is more significant for higher degrees of oxidation. The $[SbCl_6]^-$ counterions may act as a source of Cl^- anions or $SbCl_5$ which are able to cleave the cationic chain (Perry, R.; Manners, I., unpublished results). Also, in the presence of reactive oxidants such as I_2 it is also likely that Cp−Si bond cleavage occurs. Oxidation with Ag[NO_3] is reported to be nonproblematic with regard to polymer degradation (see ref 14e).

(23) (a) Foucher, D. A.; Tang, B. Z.; Manners, I. *J. Am. Chem. Soc.* **1992**, *114*, 6246. (b) Osborne, A. G.; Whiteley, R. H.; Meads, R. E. *J. Organomet. Chem.* **1980**, *193*, 345.

(24) Compton, D. L.; Rauchfuss, T. B. *Organometallics* **1994**, *13*, 4367.

(25) Manners, I. *Chem. Commun.* **1999**, *10*, 857.

(26) Pudelski, J. K.; Foucher, D. A.; Honeyman, C. H.; Macdonald, M. P.; Manners, I.; Barlow, S.; O'Hare, D. *Macromolecules* **1996**, *29*, 1894.

(27) Peckham, T. J.; Foucher, D. A.; Lough, A. J.; Manners, I. *Can. J. Chem.* **1995**, *73*, 2069.

(28) Fischer, A. B.; Kinney, J. B.; Staley, R. H.; Wrighton, M. S. *J. Am. Chem. Soc.* **1979**, *101*, 6501.

(29) Hadden, C. E.; Martin, G. E.; Krishnamurthy, V. V. *Magn. Reson. Chem.* **2000**, *38*, 143.

(30) Osborne, A. G.; Whiteley, R. H. *J. Organomet. Chem.* **1975**, *101*, C27.

(31) Pudelski, J. K.; Foucher, D. A.; Honeyman, C. H.; Lough, A. J.; Manners, I.; Barlow, S.; O'Hare, D. *Organometallics* **1995**, *14*, 2470.
(32) Sohn, Y. S.; Hendrickson, D. N.; Gray, H. B. *J. Am. Chem. Soc.* **1971**, *93*, 3603.
(33) (a) Bard, A.; Faulkner, L. R. *Electrochemical Methods*; Wiley: New York, 1980; p 229. (b) Yoshida, K. *Electrooxidation in Organic Chemistry*; Wiley: New York, 1984; p 21.
(34) Gassman, P. G.; Macomber, D. W.; Hershberger, J. W. *Organometallics* **1983**, *2*, 1470.
(35) (a) The wave spacing (E_p(ox) − E_p(red)) for **3** is significantly greater than 59 mV, which indicates that electron transfer is slow. This may be attributed to the presence of the bulky ^{t}Bu groups which hinder communication with the electrode. The tilted structure of **5** appears to favor faster electron transfer as the wave spacing is significantly less. (b) The reduced transmission may be a consequence of (i) the enforced cis arrangement of the ^{t}Bu groups in **5** where an inductive effect would generate a molecular dipole moment or (ii) the presence of a weakened Fe−Cp bond due to ring tilting.
(36) (a) Ivin, K. J.; Saegusa, T., Eds.; *Ring-Opening Polymerization*; Elsevier Applied Science: London, 1984. (b) Odian, G. *Principles of Polymerization*, 3rd ed.; Wiley & Sons: New York, 1991. (c) Allinger, N. L.; Zalkow, V. *J. Org. Chem.* **1960**, *25*, 701.
(37) (a) Temple, K.; Jäkle, F.; Sheridan, J. B.; Manners, I. *J. Am. Chem. Soc.* **2001**, *123*, 1355. (b) Ni, Y.; Rulkens, R.; Pudelski, J. K.; Manners, I. *Macromol. Rapid Commun.* **1995**, *16*, 637. (c) Reddy, N. P.; Yamashita, H.; Tanaka, M. *J. Chem. Soc., Chem. Commun.* **1995**, 2263.
(38) Gómez-Elipe, P.; Resendes, R.; Macdonald, P. M.; Manners, I. *J. Am. Chem. Soc.* **1998**, *120*, 8348.
(39) Rulkens, R.; Ni, Y.; Manners, I. *J. Am. Chem. Soc.* **1994**, *116*, 12121.
(40) (a) Ni, Y.; Rulkens, R.; Manners, I. *J. Am. Chem. Soc.* **1996**, *118*, 4102. (b) Peckham, T. J.; Massey, J. A.; Honeyman, C. H.; Manners, I. *Macromolecules* **1999**, *32*, 2830.
(41) Tanabe, M.; Manners, I. *J. Am. Chem. Soc.* **2004**, *124*, 11434.
(42) Connelly, N. G.; Geiger, W. E. *Chem. Rev.* **1996**, *96*, 877.
(43) (a) While the positions and intensities of the metal d−d transitions bands of the ferrocenium ion are insensitive to ring substitution, the LMCT band undergoes red shift upon ring substitution (see ref 32). (b) Attempted synthesis of an iron(III) silicon-bridged [1]ferrocenophane from the oxidation reaction of **5** with Ag[PF_6] (1:1) led to unexpected formation of ring-opened species [Fe(η-$C_5H_4{}^t$Bu)(η-$C_5H_3{}^t$Bu)$SiFPh_2$]$^+$[PF_6]$^-$ as confirmed by X-ray crystallography. When Ag[PF_6] is used in $CHCl_3$, CH_2Cl_2, or toluene, the hydrolysis of the [PF_6]$^-$ in the presence of traces of water is catalyzed by Ag^+ (see ref 42). The UV−vis spectrum of [Fe(η-$C_5H_4{}^t$Bu)(η-$C_5H_3{}^t$Bu)$SiFPh_2$]$^+$[PF_6]$^-$ showed a LMCT band at 660 nm, similar to that found in **7**$^+$ (Masson, G.; Lough, A. J.; Manners, I., unpublished results, 2005).
(44) O'Hare, D.; Lewis, R.; Kuhn, A.; Kurmoo, M. *Synth. Met.* **1991**, *42*, 1695.
(45) Steckhan, E. *Angew. Chem., Int. Ed. Engl.* **1986**, *25*, 683.
(46) Cowan, D. O.; LeVanda, C.; Park, J.; Kaufman, F. *Acc. Chem. Res.* **1973**, *6*, 1.
(47) Eberson, L.; Olofsson, B. *Acta Chem. Scan.* **1991**, *45*, 316.
(48) Ciminale, F.; Lopez, L.; Farinola, G. M.; Sportelli, S. *Tetrahedron Lett.* **2001**, *42*, 5685.
(49) Pangborn, A. B.; Giardello, M. A.; Grubbs, R. H.; Rosen, R. K.; Timmers, F. J. *Organometallics* **1996**, *15*, 1518.
(50) Massey, J. A.; Kulbaba, K.; Winnik, M. A.; Manners, I. *J. Polym. Sci., Part B: Polym. Phys.* **2000**, *38*, 3032.
(51) Otwinowski, Z.; Minor, W. *Methods Enzymol.* **1997**, *276*, 307.
(52) Sheldrick, G. M. *SHELXTL/PC* V5.1; Bruker Analytical X-ray Systems: Madison, WI, 1997.

MA052475M